Biosensors and Bioelectronics 144 (2019) 111621

Contents lists available at ScienceDirect

Biosensors and Bioelectronics

journal homepage: www.elsevier.com/locate/bios

A disposable fiber optic SPR probe for immunoassay

Zhigang Mai[a,1], Jinghan Zhang[b,c,d,1], Yuzhi Chen[b,c,d,*], Jiaqi Wang[b,c,d], Xueming Hong[b,c,d], Qingning Su[a], Xuejin Li[b,c,d,**]

[a] School of Medicine, Shenzhen University, Shenzhen, 518060, China
[b] College of Physics and Optoelectronic Engineering, Shenzhen University, Shenzhen, 518060, China
[c] Shenzhen Key Laboratory of Sensor Technology, Shenzhen, 518060, China
[d] Shenzhen Engineering Laboratory for Optical Fiber Sensors and Networks, Shenzhen, 518060, China

ARTICLE INFO

Keywords:
Surface plasmon resonance
Fiber optic biosensor
Immunoassay

ABSTRACT

Immunoassay can be divided into two aspects, one is immobilization of antibodies for the efficient detection of corresponding antigens, and the other is immobilization of antigens to search for antibodies which work against them. In this paper, we demonstrated these two aspects of immunoassay by using the disposable fiber optic biosensors based on surface plasmon resonance (SPR) through surface decoration with half-antibody fragments, which has been scarcely ever reported to the best of our knowledge. We first fabricated the fiber optic SPR biosensor which consists of one gold film coated single-mode fiber sandwiched by two multimode fibers. Then, we decorated the fiber optic SPR biosensors with antibody fragments and antigen fragments, respectively, and compared the specific detection performances of these two kinds of sensors. After surface decoration with half-antibody fragments, the antigen-decorated fiber probe has a demonstrated sensitivity and limit of detection of 0.9771nm/(μg/mL) and 0.1 μg/mL, respectively, which improves by 10 times compared with the performance of the antibody-decorated fiber probe. Additionally, the selective detection results indicate that our proposed biosensor can be employed as a reliable antigen detector or an effective antibody filter. Our proposed sensor has the advantages of miniaturization, low cost, simple usage, label-free detection, high efficiency and sensitivity, and can effectively avoid cross-contamination caused by reuse. Given the reliable and clean detection method for immunoassay, our work should open a new window for the utilization of miniaturized fiber optic sensors in biochemical sensing.

1. Introduction

Immunoassay is a biochemical analytical method based on the highly selective reaction between an antibody and an antigen, which is embodied in two aspects. One is immobilization of antibodies for the efficient detection of corresponding antigens. It is widely used for the early diagnosis of cancers, tumors, autoimmune diseases and the detection of allergens (Wang et al., 2010). The other is immobilization of antigens to search for antibodies that work against them. It is an effective mechanism that contributes to the development of new drugs such as designing inhibitors for neutralization of hepatitis A virus (Cao et al., 2019). Immunoassay is of particular importance for the research and development of medicine and life sciences. Therefore, a number of methods, such as immunofluorescence assay (Ren et al., 2015), radioimmunoassay (Barta et al., 2017), enzyme-linked immunosorbent assay (ELISA) (Kjelgaard-Hansen et al., 2003) and chemiluminescence immunoassay (Kricka, 2003) have been developed for immunoassay currently. Although these analytical methods show high sensitivity and selectivity, they still have some limitations, for example, time-consumption, indirect detection format, semi-quantitative detection, expensive equipment, and the requirement for skilled operators. Consequently, there is an urgent need for the development of simple, rapid, low-cost, convenient, highly sensitive methods for immunoassay (Lu et al., 2016). Fiber optic biosensors (Chen et al., 2016) and nanowire field effect transistor biosensors (Stern et al., 2007) can be candidates.

In general, the reaction of antibody and antigen would lead to a tiny refractive index (RI) change in the reaction environment, which also occurs in other reactions of biochemical molecules. And there is an optical analysis method, i.e. surface plasmon resonance (SPR), that is extremely sensitive to tiny RI changes and suitable for the applications

* Corresponding author. College of physics and optoelectronic engineering, Shenzhen University, Shenzhen, 518060, China.
** Corresponding author. College of physics and optoelectronic engineering, Shenzhen University, Shenzhen, 518060, China.
E-mail addresses: chenyuzhi@szu.edu.cn (Y. Chen), lixuejin@szu.edu.cn (X. Li).
[1] These authors contributed equally to this work and should be considered as co-first authors.

https://doi.org/10.1016/j.bios.2019.111621
Received 24 June 2019; Received in revised form 19 August 2019; Accepted 20 August 2019
Available online 22 August 2019
0956-5663/

in biochemical analysis. By grafting SPR technology into a suitable fiber optic, a miniaturized, cost-effective, easy-to-use and sensitive biosensor can be fabricated for the immunoassay. For the fiber optic SPR sensor, common types are D-shaped fiber SPR sensors (Zainuddin et al., 2019), hetero-core fiber SPR sensors (Iga et al., 2005), multimode fiber SPR sensors (Wang et al., 2017a) and photonic crystal fiber SPR sensors (Xie et al., 2017). In fact, in recent years, some applications in molecule interaction analysis and concentration detection of the target molecule have been reported by employing fiber optic SPR biosensors due to their advantages in volume and operation (Sharma et al., 2018; Gupta and Kant, 2018). For example, Daems D. et al. reported a fiber optic SPR biosensor based competitive inhibition assay to detect progesterone in complex biological fluids. Their modified sensor achieved a detection limit of 0.5 ng/mL in 2-fold diluted bovine milk (Daems et al., 2017). In 2017, Lu J.et al. presented a short-time immunoassay (10 min) using a fiber optic SPR biosensor for determining infliximab concentrations in a variety of matrixes (Lu et al., 2017). In 2017, Wang W. et al. demonstrated a novel fiber optic SPR biosensor for the specific detection of C-reactive protein (CRP) by utilizing dopamine as a crosslinking agent to immobilize the anti-CRP monoclonal antibody. Their detection concentration ranges from 0.01 to 20 μg/mL with a sensitivity of 1.17 nm per lg(μg/mL) (Wang et al., 2017a). Recently, Wang Q. et al. proposed a graphene oxide/silver coated fiber optic SPR biosensor to detect Human IgG, their sensor reached a sensitivity of 0.4985 nm/(μg/mL) and a low limit of detection of 0.04 μg/mL (Wang and Wang, 2018). More importantly, compared with the traditional immunoassay methods, the main advantages of fiber optic SPR biosensors are their ability to achieve label-free detection of analytes, so as to overcome conjugate interference.

Without labeling process, the use of fiber optic SPR biosensors is simpler and more efficient than those of traditional immunoassays. Further, how to decorate the specific detection layer onto the sensor surface and improve the detection performance have become the key issues for a fiber optic SPR biosensor. Taking the antibody-decorated biosensor for the detection of the corresponding antigen as an example. The more efficient immobilization of antibodies, the more target molecules will be captured. Accordingly, in order to improve the antibody immobilization efficiency onto the sensor surface, there are several methods as possible candidates, for instance, employing protein A or protein G as a sub-layer protein to connect biotin to avidin (Ko et al., 2009; Maisonneuve et al., 2015), the sensor surface is functionalized with 3-aminopropyltriethoxysilane (APTES) and subsequently biotinylated for the selective immobilization of streptavidin. (Williams et al., 2012), depositing a dopamine self-polymerization layer as a bio-adhesive (Shi et al., 2015; Wang et al., 2017a), combining amine groups with the 1-ethyl-3-(3-(dimethylamino)propyl)-carbo-diimidehydrochloride/N-hydroxysulfosuccinimide (EDC/NHS) activated carboxyl group (Park et al., 2014), directly immobilizing antibodies with sulfhydryl groups on a gold film (Billah et al., 2010), etc. Among these methods, the covalent binding of thiol with gold is a direct method for protein (antibody) to combine onto the sensor surface with gold film, which should be a sensitivity-enhanced method for the gold-based fiber optic SPR sensor, since the antigen-antibody reaction will be much closer to the sensor surface without any additional adhesive layers. There are two ways to obtain an antibody taking sulfhydryl groups. One is to decorate it with a compound containing a sulfhydryl group (Wang et al., 2015, Wang et al., 2017b) However, antibodies are randomly decorated in this way, some of them may be unable to recognize analyte due to the steric hindrance of binding sites. The other way is to open the disulfide bond between the antibody chains to obtain thiol sites (Domen et al., 1990; Lu et al., 1996). Compared to the former, the free-SHs, i.e. sulfhydryl groups, come from the later way have fixed number and certain sites which are far from antibody recognition sites. Although disulfide bonds play an important role in maintaining the structure and activity of antibody molecules, especially the disulfide bonds between heavy and light chains. Fortunately, the disulfide bridge present in the hinge region of the Immunoglobulin G (IgG) can be subject to be opened according to a controlled reduction procedure to generate half-antibody fragments which act as fragments of antigen binding (Fab) (Makaraviciute et al., 2016). The approach of immobilizing half-antibody fragments on gold film should result in higher accessibility for antigens, less variable interaction kinetics, and thereby, improved analyte recognition, since the half-antibody recognition sites are freely available through the oriented immobilization of free-SHs on gold film (Bonroy et al., 2006; Lu et al., 1996; Sharma and Mutharasan, 2013).

In this study, a novel disposable fiber optic SPR probe for immunoassay is experimentally proposed by employing an approach of half-antibody fragment immobilization onto the gold-based sensor surface. We fabricated fiber optic SPR biosensors with multimode fiber-single mode fiber-multimode fiber (M-S-M) structure to compare the two kinds of immunoassay, namely, one using the antibody-decorated fiber probe for the antigen detection, and the other employing the antigen-decorated fiber probe for the antibody detection. To verify the feasibility of these assays, mouse IgG (M-IgG) and goat anti-mouse IgG (GAM-IgG) were selected as the antigen and antibody, respectively. In the process of biological decoration and detection, the concentration of the GAM-IgG fragments immobilized on the sensor surface was firstly optimized to achieve the satisfactory performance for the proposed fiber probe, so does the M-IgG fragments. Then we evaluated the sensitivities of the GAM-IgG-decorated fiber probe and M-IgG-decorated fiber probe, respectively. Finally, the specific detection ability of these two kinds of fiber probes was also investigated. Our work successfully implements a disposable fiber probe for immunoassay, which is of miniaturization, low cost, simple usage, high efficiency, and sensitivity, and can avoid cross-contamination caused by reuse.

2. Experiment and method

2.1. Fabrication of the fiber optic SPR biosensor and its sensing system

At the beginning of the experiment, we first prepared disposable fiber optic SPR biosensors for the follow-up study on immunoassay. As described at the bottom of Fig. 1, the proposed biosensor with hetero-core fiber, i.e. M-S-M, structure was fabricated by splicing a single mode fiber (SMF, 9 μm core and 125 μm cladding diameters) between two multimode fibers (MMF, 62.5 μm core and 125 μm cladding diameters), and therefore the cladding modes of SMF can be excited through butting hetero core fibers. This type of hetero-core fiber sensor had been proposed and evaluated positively in previous research for its sensitivity and the high measurement precision (Goh et al., 2013; Iga et al., 2005). Here the SMF region was set to 12-mm length and gently cleaned by the anhydrous ethanol and then distilled water to remove the residual dust. After completed the clean surface of the SMF region, the JGP450A magnetron sputtering fiber coating device (SKY Technology Development Inc.) was employed to deposit a gold film onto the SMF region. In this way, a number of proposed fiber probes were fabricated for the subsequent immune decoration and detection. Gold films, whose plasma are excited by cladding modes, were uniformly controlled at the same thickness of 45 nm to ensure the plasma excitation efficiency (Chen et al., 2016) and the consistency of the disposable biosensors.

Next, a sensing system designed for the proposed biosensor was set up, as illustrated in Fig. 1, which includes a broadband light source (Thorlabs Inc., SLS201/L, 360–2600 nm), a spectrometer (USB 4000, Ocean Optics Inc.,200–1100 nm), a computer and the fiber optic SPR biosensor. To connect the light source, the proposed biosensor and the spectrometer, transmission fibers of MMF were employed. When the biosensor is in operation, the incident light firstly propagates through the fiber core from MMF to the SMF. Then a part of the incident light is coupled into the SMF cladding from the MMF core. Finally, the incident light reveals into the gold film in the form of the evanescent field. When the parallel component of the incident light wave vector matches that of the surface plasmon wave, strong absorption of light occurs. As a result,

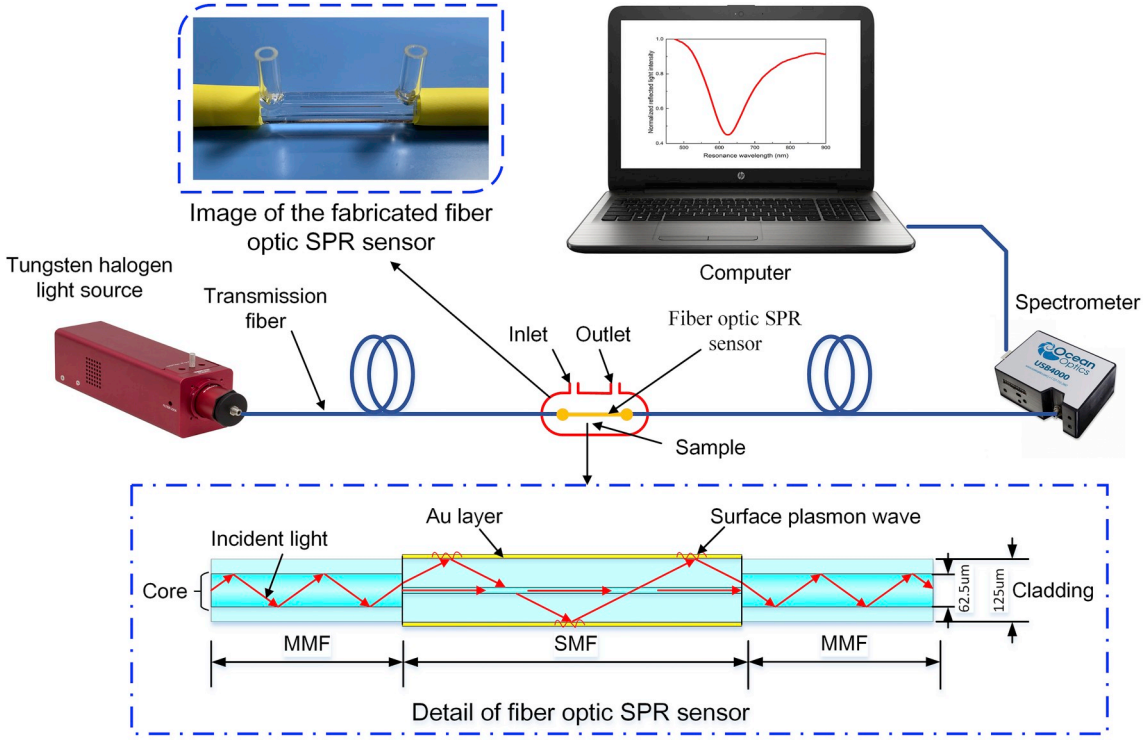

Fig. 1. Schematic diagram of the sensing system.

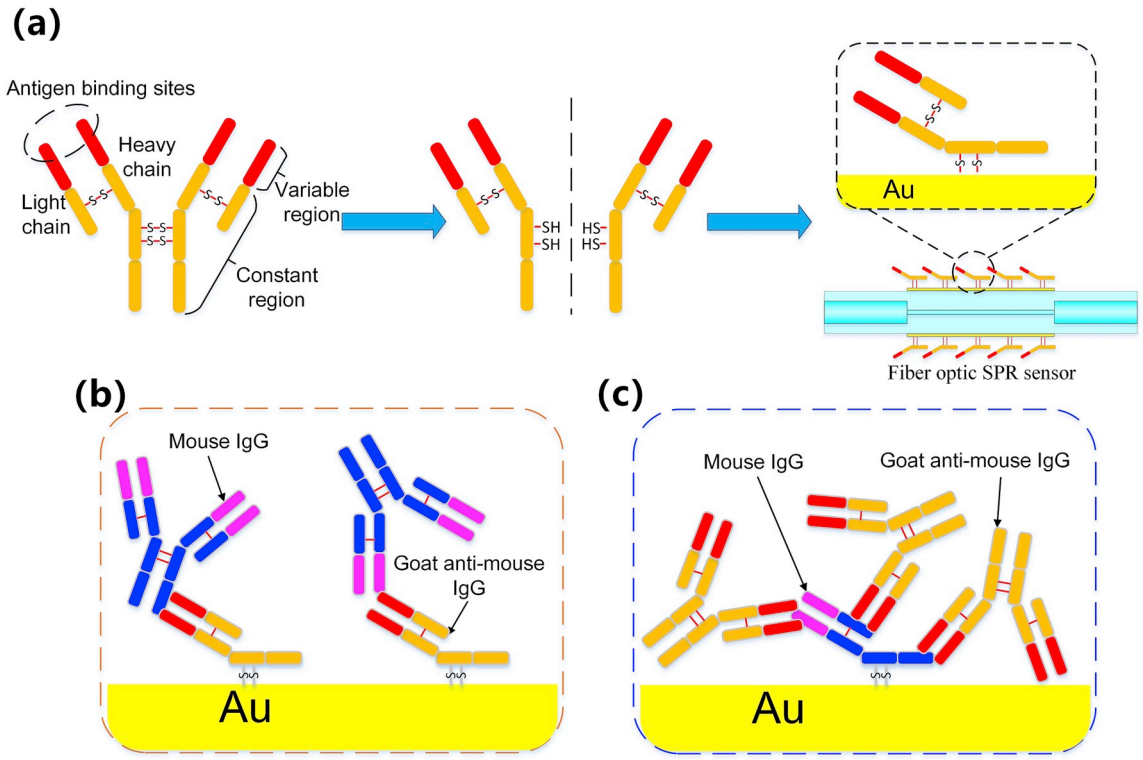

Fig. 2. Surface decoration and specific detection of the fiber optic SPR biosensor: (a) the decoration process of a GAM-IgG-decorated fiber probe; (b) the M-IgG detection by using a GAM-IgG-decorated fiber probe; (c) the GAM-IgG detection by employing an M-IgG-decorated fiber probe.

an SPR dip at a particular wavelength, which is known as resonance wavelength, appears in the output spectrum signal (Velázquez-González et al., 2017; Zhao et al., 2018). When the external RI changes or antigen-antibody binding reaction happens on the sensor surface, the SPR dip will shift accordingly. The signal captured can be shown and monitored by the computer connected with the spectrometer.

2.2. Materials of the biological decoration and detection

The purified M-IgG and GAM-IgG, i.e. the antigen and antibody in this experiment, respectively, were purchased from Origene Company, 2-mercaptoethylamine (2-MEA), Ethylenediaminetetraacetic acid disodium salt (EDTA-2Na), Bovine Serum Albumin (BSA), Ovalbumin

(OVA) and Casein were purchased from Sigma-Aldrich Company. Phosphate buffered saline (PBS, 10 mM, pH 7.4, 1.76 mM KH_2PO_4, 10.14 mM $Na_2HPO_4{\cdot}12H_2O$, 136.75 mM NaCl, 2.68 mM KCl) are prepared with ultra-pure water. All the chemicals used in this experiment are of analytical reagent grade.

2.3. Preparation of GAM-IgG-decorated and M-IgG-decorated fiber probes

In order to prepare half-antibody fragments to decorate the sensor surface for the specific detection, we first treated purified antibody (5 mg/mL) with 50 mM 2-MEA, in PBS with 10 mM EDTA-2Na, pH 6.0 for 4.0 h. This approach selectively reduced the disulfide bonds in the hinge regions of IgG (Billah et al., 2008; Hermanson, G.T., 2008), thus forming two monovalent IgGs, i.e. half-antibody fragments, bearing 1–2 free sulfhydryl groups. The reduced IgGs were then ultrafiltered with Millipore (30K) for 5 times in an anaerobic 1 × PBS to remove excess 2-MEA. Next, the reduced IgGs were concentrated and stored anaerobically at −20 °C for the further decoration of the proposed fiber probes. Finally, the sensing region of the proposed fiber probe was immersed in the solution of reduced IgGs (diluted with PBS buffer, pH = 7.4) for 48 h at 4°C for the self-assembly of free-SHs (sulfhydryl groups) on the gold film. After sufficiently washed with PBS, the GAM-IgG-decorated fiber probe was ready for the M-IgG detection. The decoration process of the GAM-IgG-decorated fiber probe is shown in Fig. 2a. In the same way, we also prepared the M-IgG-decorated fiber probe for the GAM-IgG detection.

2.4. Immunoassays

Immunoassays in this paper are divided into two parts, one is the M-IgG detection by using a GAM-IgG-decorated fiber probe, as shown in Fig. 2b; the other is the GAM-IgG detection by employing an M-IgG-decorated fiber probe, as described in Fig. 2c. Both of the concentrations used for decoration (GAM-IgG decoration and M-IgG decoration) were first optimized by respectively measuring the corresponding target molecule at a fixed concentration. Afterward, we evaluated the sensitivity of the GAM-IgG-decorated and M-IgG-decorated fiber probes in measuring their corresponding target molecules with different concentration levels, respectively. Finally, selectivities of these two kinds of fiber probes were also investigated by detecting different types of proteins, i.e. GAM-IgG/M-IgG, BSA, OVA, Casein, in two concentrations of 10 μg/mL and 100 μg/mL, respectively. It is worth to mention that all the assays in this paper were performed by using disposable fiber probes, and each assay was repeated more than 3 times.

3. Result and discussion

3.1. Optical characteristics of the fiber optic SPR biosensor

As the SPR phenomenon is sensitive to RI change which is directly related to the binding of antigens and antibodies, we first evaluated the RI sensitivity of the prepared fiber optic SPR biosensor before its GAM-IgG or M-IgG decoration. The sensing region of a proposed fiber probe was immersed into the NaCl solutions with different RI ranging from 1.3342 to 1.3762 (calibrated by WYA-2S Abbe refractometer at a room temperature of 25 °C) to generate corresponding resonance dips, as shown in Fig. 3a. With the increase of RI, the resonance dip has a red shift. The linear relationship between the resonance wavelength, i.e. the bottom point of the resonance dip, and RI is described in Fig. 3b, which indicates that the RI sensitivity of the proposed fiber probe is obtained to be 1959.6 nm/RIU in a RI range of 1.3342–1.3762, totally enough for bioassay (Shi et al., 2015; Wang et al., 2017a). In addition, to ensure the consistency of our biosensors for the following immunoassays, all the proposed fiber probes with same preparation parameters were selected by measuring deionized water (RI = 1.3342), 1 × PBS solution (RI = 1.3362) and then 4 × PBS solution (RI = 1.3422) for the uniform sensitivity. At the end of the fiber probe selection, we chose fiber probes with a sensitivity relative standard deviation (RSD) less than 8% for the subsequent experiments.

3.2. M-IgG detection by using a GAM-IgG-decorated fiber probe

The proposed GAM-IgG-decorated fiber probe was employed for the specific detection of corresponding M-IgG herein. To achieve the satisfactory performance of the proposed fiber probe, the effective immobilization of the GAM-IgG on the sensor surface is crucial. Consequently, it is necessary to optimize the decoration concentration of GAM-IgG fragments first. Several concentrations (25 μg/mL, 50 μg/mL, 75 μg/mL, 100 μg/mL and 125 μg/mL) of the treated GAM-IgG were prepared by diluted with PBS buffer for the decoration on sensor surface (decoration process see Section 2.3). Then the GAM-IgG-decorated disposable fiber probes were evaluated by measuring 50 μg/mL M-IgG, whose results are shown in Fig. 4a. The selection criterion is based on the resonance wavelength shift before and after the M-IgG detection (the larger shift, the better). As the concentration of the treated GAM-IgG increases, the maximum resonance wavelength shift is obtained to be 4.65 nm at 50 μg/mL, while the other resonance wavelength shifts are basically maintained below 3 nm. Here the corresponding standard deviation of each experimental point is described as orange error bar. The insufficiency of resonance wavelength shift at an GAM-IgG-decorated concentration of 25 μg/mL is attributed to lack of GAM-IgG fragments to capture target molecules. And when the concentration of treated GAM-IgG exceeds 50 μg/mL, the random self-assembly makes the specific detection layer become thicker, which results in blocking some of the recognition sites in GAM-IgG fragments, thus reducing the detection efficiency. Ultimately, it can be determined that the GAM-IgG-decorated concentration of 50 μg/mL is an optimal value for the M-IgG detection by our proposed fiber probe.

Following the optimization of specific detection layer, we used the optimized biosensors to detect M-IgGs with different concentrations of 5 μg/mL, 10 μg/mL, 20 μg/mL, 50 μg/mL and 100 μg/mL, respectively. Fig. 4b demonstrates the experimental results of repeated measures, it is observed that our biosensors exhibit a satisfactory linear response to the M-IgG in a concentration range of 5–100 μg/mL. Here sensitivity (S) and limit of detection (LOD) are introduced to estimate the performance of the optimized biosensor. S describes the change rate of resonance wavelength (λ_R) with the concentration (n) variation of the target molecule, which can be defined as:

$$S = \frac{d\lambda_R}{dn} \tag{1}$$

And LOD reflects the minimum concentration of the target molecule that a biosensor can detect. We obtained LOD though an approach of experimental measurements. After several times of measurements in the background solution, i.e. 0 μg/mL M-IgG, the mean value of the blank response fluctuation was obtained to be 0.2 nm in resonance wavelength shift. Then we diluted the M-IgG concentration continuously so that the biosensor response was closer to 0.2 nm. The final LOD was the M-IgG concentration with the closest response that was slightly higher than 0.2 nm.

Finally, S and LOD of the optimized GAM-IgG-decorated biosensor are obtained to be 0.078nm/(μg/mL) and 1 μg/mL, respectively, through the calculation and analysis of experimental data.

3.3. GAM-IgG detection by employing an M-IgG-decorated fiber probe

The same operation as Section 3.2, the decoration concentration of M-IgG fragments, should be optimized first to achieve an M-IgG-decorated fiber probe with a satisfactory performance for the specific detection of the corresponding GAM-IgG. Also, several concentrations (5 μg/mL, 10 μg/mL, 20 μg/mL, 50 μg/mL and 100 μg/mL) of the treated M-IgG were prepared by diluted with PBS buffer. After surface

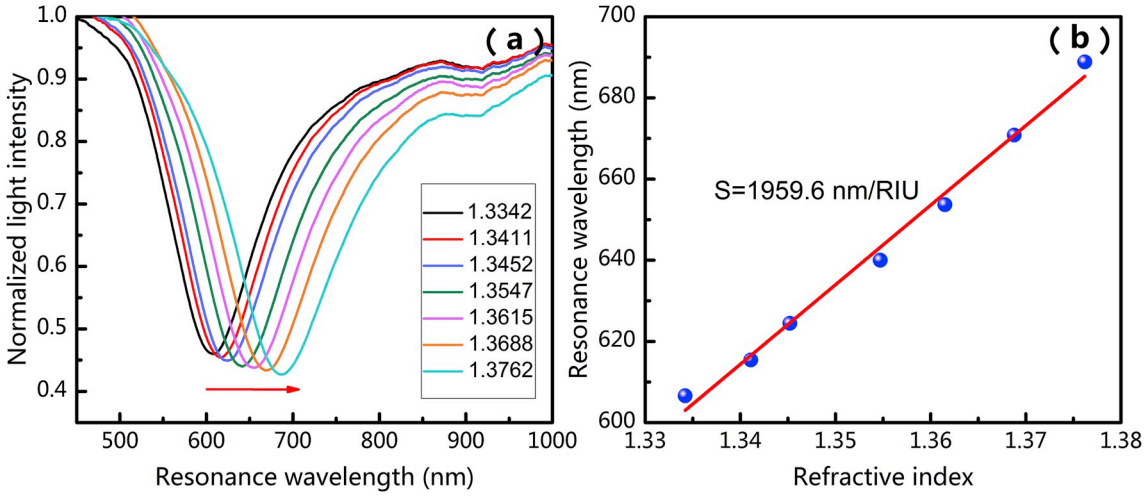

Fig. 3. Performance evaluation of the fiber optic SPR biosensor: (a) normalized spectra in measuring NaCl solutions with different RI values; (b) experimental measurement of the external RI-dependent resonance wavelength.

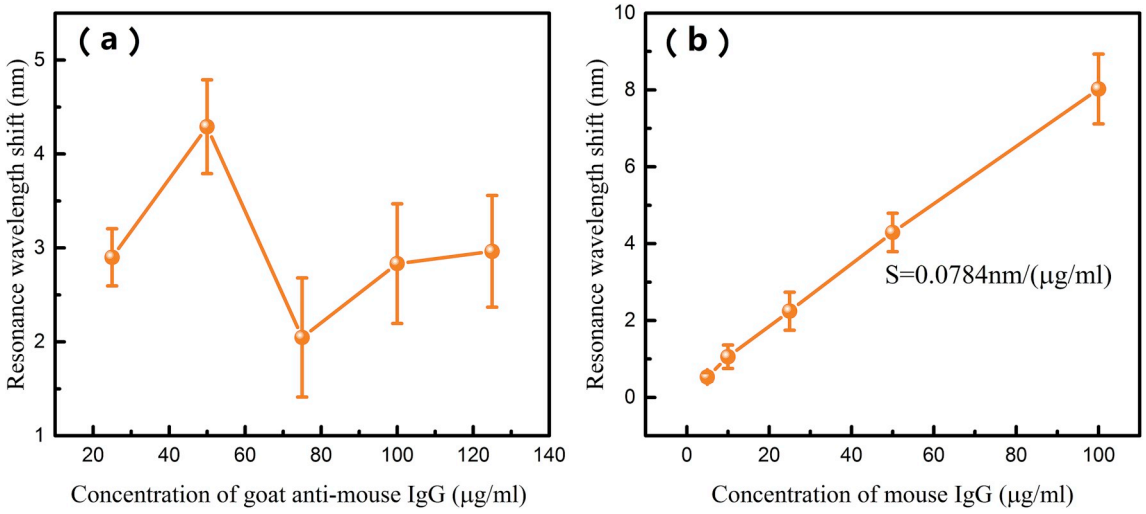

Fig. 4. (a) Resonance wavelength shifts of the proposed fiber probes with different GAM-IgG-decorated concentrations by measuring 50 μg/mL M-IgG. (b) Resonance wavelength shifts of the proposed fiber probes with a fixed GAM-IgG-decorated concentration of 50 μg/mL by measuring different concentrations of M-IgG.

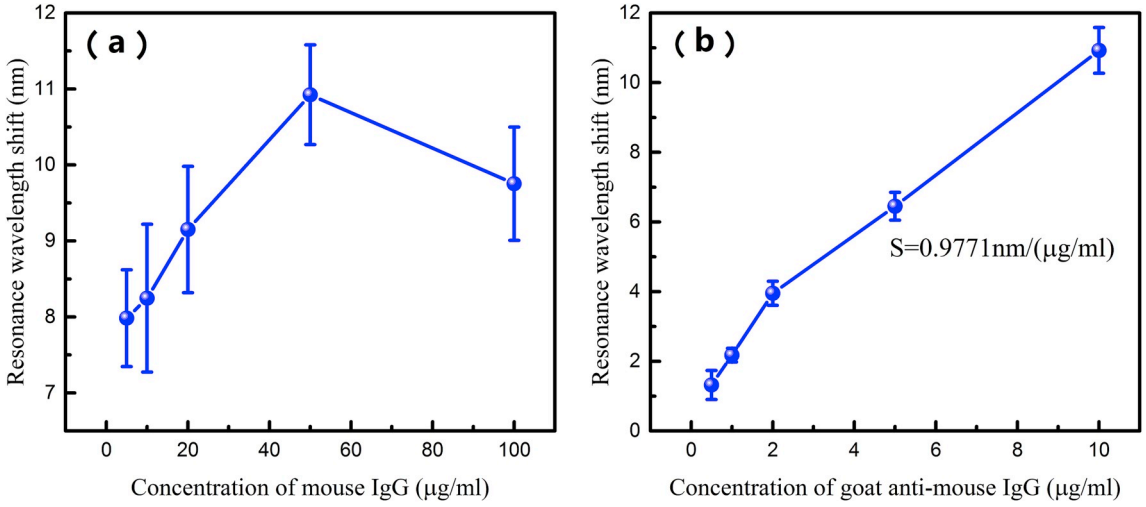

Fig. 5. (a) Resonance wavelength shifts of the proposed fiber probes with different M-IgG-decorated concentrations by detecting 10 μg/mL GAM-IgG. (b) Resonance wavelength shifts of the proposed fiber probes with a fixed M-IgG-decorated concentration of 50 μg/mL by detecting different concentrations of GAM-IgG.

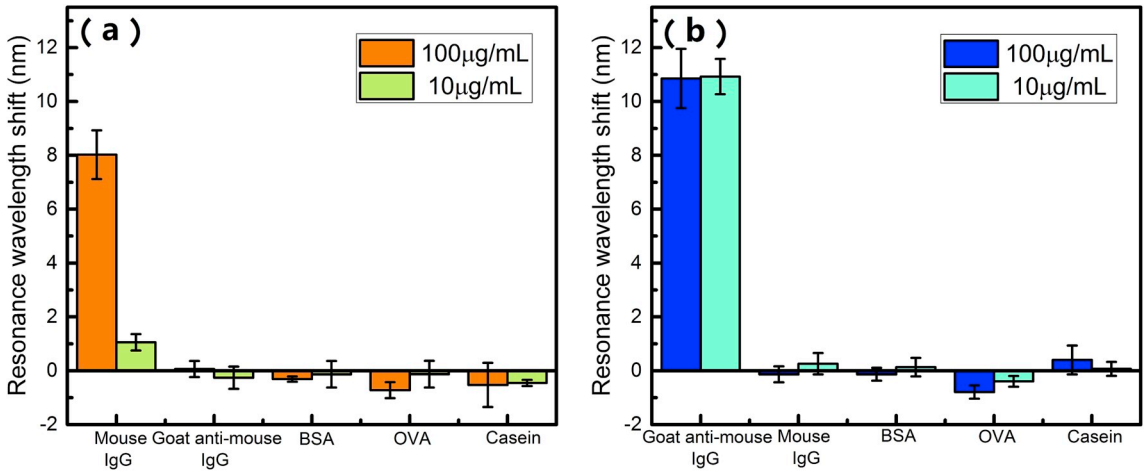

Fig. 6. Selectivity of the proposed biosensor decorated with (a) GAM-IgG and (b) M-IgG. Different proteins (GAM-IgG, M-IgG, BSA, OVA, and Casein) with a low concentration of 10 μg/mL and high concentration of 100 μg/mL are chosen for the selective detection. The error bars represent the standard deviations from three dependent assays.

decoration with M-IgGs of different concentrations, the proposed biosensors were next evaluated by detecting 10 μg/mL GAM-IgG, whose results are shown in Fig. 5a. With the increasing concentration of the treated M-IgG, the resonance wavelength shift first increases and then decreases, the maximum value is obtained to be 11.52 nm at an M-IgG-decorated concentration of 50 μg/mL, while the corresponding standard deviation of each experimental point is described as blue error bar. The resonance wavelength shift shows that the detection ability of target antibodies improves with the increase of the M-IgG-decorated concentration within 50 μg/mL. However, when the concentration exceeds 50 μg/mL, the random self-assembly causes the supersaturated accumulation of M-IgG fragments, which thickens the specific detection layer and reduces its detection efficiency. Considering that the sensitive M-IgG-decorated fiber probe can improve the efficiency of finding corresponding antibodies. We choose the M-IgG-decorated concentration of 50 μg/mL in the following experiments.

Detecting target antibodies with different concentrations of 0.5 μg/mL, 1 μg/mL, 2 μg/mL, 5 μg/mL and 10 μg/mL by the optimized M-IgG-decorated biosensors, Fig. 5b demonstrates their experimental results. One can observe that the resonance wavelength shift increases with the increasing concentration of GAM-IgG. At the same time, its change rate decreases gradually due to the trend of detection saturation of target molecules. After further calculation and analysis of the experimental data in this section, the average *S* and *LOD* of the optimized M-IgG-decorated biosensor are obtained to be 0.9771nm/(μg/mL) and 0.1 μg/mL, respectively.

By comparing the results of GAM-IgG-decorated and M-IgG-decorated fiber probes, one can find that *S* of the M-IgG-decorated fiber probe is more than 10 times greater than that of GAM-IgG-decorated fiber probe. This is mainly attributed to the number of effective recognition sites in the molecules used for decoration. An intuitive illustration indicates, shown in Fig. 2b and c, that the effective recognition sites of a GAM-IgG are only the variable regions which are highlighted in red, while there are multiple antigenic determinants in an M-IgG which can be recognized by the corresponding target molecules (goat anti-mouse IgGs are polyclonal antibodies to the mouse IgG). Thus, by immobilizing a GAM-IgG and an M-IgG on the sensor surface, the ability of the M-IgG to capture target molecules is much greater than that of the GAM-IgG herein. Comparing graphs (a) and (b) in Figs. 4 and 5, we can observe that error bars in graphs (a) are greater than those in graphs (b). This indicates that the exploration of the conditions of the decoration layer would bring a greater uncertainty impact on our proposed biosensors since the decoration layer is much closer to the sensor surface than target molecules. And once the decoration layer is determined and the proposed biosensors are uniformly decorated, their accuracy will become more reliable.

The study in these two sections proves that the self-assembly of half-antibody fragments on the sensor surface is a feasible approach for decoration on fiber optic SPR biosensors. Moreover, our proposed biosensor can be employed as an antigen detector or an antibody filter through appropriate decoration, which may bring new vitality to immunoassay.

3.4. Selectivity of the proposed biosensors

At the end of the experiment, the selectivities of the GAM-IgG-decorated and M-IgG-decorated fiber probes were investigated by measuring different kinds of proteins, respectively. Fig. 6a depicts the results of the biosensor decorated with GAM-IgG, satisfactory selectivity results are obtained and the significant different responses in detecting 10 μg/mL and 100 μg/mL target molecules is attributed to the unsaturated detection in this concentration range. While Fig. 6b also demonstrates apparent selectivity to the target molecule for the biosensor decorated with M-IgG. However, the responses to target molecules of 10 μg/mL and 100 μg/mL are basically indistinguishable. It is mainly because 10 μg/mL GAM-IgG is the upper limit for the proposed M-IgG-decorated biosensor and the concentration increase above 10 μg/mL no longer affects the response.

Selectivity results reveal that the responses of the proposed biosensors are caused by the specific binding of molecules rather than their concentrations (Shi et al., 2015). In addition, using disposable fiber probes for the target molecular screening experiments can greatly improve detection efficiency and effectively avoid cross-contamination caused by sensor reuse. We demonstrate a new method of simplicity, convenience, reliability, and label-free for immunoassay.

4. Conclusion

In summary, a disposable fiber optic SPR biosensor with M-S-M structure was proposed for immunoassay in this paper, which is sensitivity, reliable, user-friendly, cost-effective, and most importantly, avoidable for the cross-contamination caused by reuse. Two parts of immunoassay were investigated, i.e. using the GAM-IgG-decorated fiber probe for the M-IgG detection, and employing the M-IgG-decorated fiber probe for the GAM-IgG detection. After optimization, *S* and *LOD* of the GAM-IgG-decorated fiber probe are obtained to be 0.078nm/(μg/mL) and 1 μg/mL, respectively. While those of the M-IgG-decorated fiber probe is obtained to be 0.9771nm/(μg/mL) and 0.1 μg/mL, respectively. It should be noted that *S* and *LOD* in this study are obtained through the experiment measurements, which includes the error of the

whole system and the influence of the environment, and has practical application value. The 10 times detection capability of the M-IgG-decorated fiber probe with respect to that of the fiber probe decorated with GAM-IgG indicates that the improvement of decorated molecules and methods can effectively improve the performance of our biosensors. Moreover, after the selectivity study, the experimental results show that our proposed biosensor can be employed as a reliable antigen detector or an effective antibody filter, which may bring new vitality to immunoassay.

In this work, *S* and *LOD* of our proposed fiber probe are still insufficient in detecting smaller amounts of target molecules. Next, we will study methods to improve the detection efficiency of the bio-decorated layer and develop a more sensitive fiber optic SPR biosensor.

CRediT authorship contribution statement

Zhigang Mai: Data curation. **Jinghan Zhang:** Formal analysis. **Yuzhi Chen:** Conceptualization. **Jiaqi Wang:** Writing - review & editing. **Xueming Hong:** Project administration. **Qingning Su:** Investigation. **Xuejin Li:** Funding acquisition.

Declaration of competing interest

The authors declare that they have no known competing financial interests or personal relationships that could have appeared to influence the work reported in this paper.

Acknowledgments

This work is jointly supported by the National Natural Science Foundation of China (Grant No. 61775149 and 61805164), Shenzhen Science and Technology Project (Grant No. JCYJ20160226192754225), Natural Science Foundation of Guangdong (2016A030313059), and Science and Technology plan project of Guangdong(2017A010101018).

Appendix A. Supplementary data

Supplementary data to this article can be found online at https://doi.org/10.1016/j.bios.2019.111621.

References

Barta, P., Janousek, J., Zilkova, K., Trejtnar, F., 2017. J. Label. Comp. Radiopharm. 60, 80–86. https://doi.org/10.1002/jlcr.3478.
Billah, M., Hays, H.C.W., Millner, P.A., 2008. Microchim. Acta 160, 447–454. https://doi.org/10.1007/s00604-007-0793-0.
Billah, M.M., Hodges, C.S., Hays, H.C.W., Millner, P.A., 2010. Bioelectrochemistry 80, 49–54. https://doi.org/10.1016/j.bioelechem.2010.08.005.
Bonroy, K., Frederix, F., Reekmans, G., Dewolf, E., De Palma, R., Borghs, G., Declerck, P., Goddeeris, B., 2006. J. Immunol. Methods 312, 167–181. https://doi.org/10.1016/j.jim.2006.03.007.
Cao, L., Liu, P., Yang, P., Gao, Q., Li, H., Sun, Y., Zhu, L., Lin, J., Su, D., Rao, Z., Wang, X., 2019. PLoS Biol. 17, e3000229. https://doi.org/10.1371/journal.pbio.3000229.
Chen, Y., Yu, Y., Li, X., Zhou, H., Hong, X., Geng, Y., 2016. Sens. Actuators B Chem. 226, 412–418. https://doi.org/10.1016/j.snb.2015.09.056.
Daems, D., Lu, J., Delport, F., Mariën, N., Orbie, L., Aernouts, B., Adriaens, I., Huybrechts, T., Saeys, W., Spasic, D., Lammertyn, J., 2017. Anal. Chim. Acta. https://doi.org/10.1016/j.aca.2016.11.005.
Domen, P.L., Nevens, J.R., Mallia, A.K., Hermanson, G.T., Klenk, D.C., 1990. J. Chromatogr. A 510, 293–302. https://doi.org/10.1016/S0021-9673(01)93763-X.
Goh, L.S., Anoda, Y., Kazuhiro, W., Shinomiya, N., 2013. Sensors (Switzerland) 14, 468–477. https://doi.org/10.3390/s140100468.
Gupta, B.D., Kant, R., 2018. Opt. Laser. Technol. 101, 144–161. https://doi.org/10.1016/j.optlastec.2017.11.015.
Hermanson, G.T., 2008. Bioconjugate Techniques, second ed. Academic Press Inc, pp. 792–793.
Iga, M., Seki, A., Watanabe, K., 2005. Sens. Actuators B Chem. 106, 363–368. https://doi.org/10.1016/j.snb.2004.08.017.
Kjelgaard-Hansen, M., Jensen, A.L., Kristensen, A.T., 2003. Evaluation of a commercially available human C-reactive protein (CRP) turbidometric immunoassay for determination of canine serum CRP concentration. Vet. Clin. Pathol. 32, 81–87.
Ko, S., Park, T.J., Kim, H.S., Kim, J.H., Cho, Y.J., 2009. Biosens. Bioelectron. 24, 2592–2597. https://doi.org/10.1016/j.bios.2009.01.030.
Kricka, L.J., 2003. Anal. Chim. Acta 500, 279–286. https://doi.org/10.1016/S0003-2670(03)00809-2.
Lu, B., Smyth, M.R., O'Kennedy, R., 1996. Analyst 121, 29–32. https://doi.org/10.1039/an996210029r.
Lu, J., Van Stappen, T., Spasic, D., Delport, F., Vermeire, S., Gils, A., Lammertyn, J., 2016. Biosens. Bioelectron. 79, 173–179. https://doi.org/10.1016/j.bios.2015.11.087.
Lu, J., Spasic, D., Delport, F., Van Stappen, T., Detrez, I., Daems, D., Vermeire, S., Gils, A., Lammertyn, J., 2017. Anal. Chem. 89, 3664–3671. https://doi.org/10.1021/acs.analchem.6b05092.
Maisonneuve, M., Valsecchi, C., Wang, C., Brolo, A.G., Meunier, M., 2015. Biosens. Bioelectron. 63, 80–85. https://doi.org/10.1016/j.bios.2014.06.018.
Makaraviciute, A., Jackson, C.D., Millner, P.A., Ramanaviciene, A., 2016. J. Immunol. Methods 429, 50–56. https://doi.org/10.1016/j.jim.2016.01.001.
Park, J.H., Byun, J.Y., Mun, H., Shim, W.B., Shin, Y.B., Li, T., Kim, M.G., 2014. Biosens. Bioelectron. 59, 321–327. https://doi.org/10.1016/j.bios.2014.03.059.
Ren, Z.Q., Liu, T.C., Zhuang, S.H., Lin, G.F., Hou, J.Y., Wu, Y.S., 2015. PLoS One 10. https://doi.org/10.1371/journal.pone.0130481.
Sharma, H., Mutharasan, R., 2013. Anal. Chem. 85, 2472–2477. https://doi.org/10.1021/ac3035426.
Sharma, A.K., Pandey, A.K., Kaur, B., 2018. Opt. Fiber Technol. 43, 20–34. https://doi.org/10.1016/j.yofte.2018.03.008.
Shi, S., Wang, L., Su, R., Liu, B., Huang, R., Qi, W., He, Z., 2015. Biosens. Bioelectron. 74, 454–460. https://doi.org/10.1016/j.bios.2015.06.080.
Stern, E., Wagner, R., Sigworth, F.J., Breaker, R., Fahmy, T.M., Reed, M.A., 2007. Nano Lett. 7, 3405–3409. https://doi.org/10.1021/nl071792z.
Velázquez-González, J.S., Monzón-Hernández, D., Moreno-Hernández, D., Martínez-Piñón, F., Hernández-Romano, I., 2017. Sens. Actuators B Chem. 242, 912–920. https://doi.org/10.1016/j.snb.2016.09.164.
Wang, Q., Wang, B.T., 2018. Sens. Actuators B Chem. 275, 332–338. https://doi.org/10.1016/j.snb.2018.08.065.
Wang, X., Li, Y., Wang, H., Fu, Q., Peng, J., Wang, Y., Du, J., Zhou, Y., Zhan, L., 2010. Biosens. Bioelectron. 26, 404–410. https://doi.org/10.1016/j.bios.2010.07.121.
Wang, X., Mei, Z., Wang, Y., Tang, L., 2015. Talanta 136, 1–8. https://doi.org/10.1016/j.talanta.2014.11.023.
Wang, W., Mai, Z., Chen, Y., Wang, J., Li, L., Su, Q., Li, X., Hong, X., 2017a. Sci. Rep. 7, 1–8. https://doi.org/10.1038/s41598-017-17276-3.
Wang, X., Mei, Z., Wang, Y., Tang, L., 2017b. Beilstein J. Nanotechnol. 8, 372–380. https://doi.org/10.3762/bjnano.8.39.
Williams, E.H., Davydov, A.V., Motayed, A., Sundaresan, S.G., Bocchini, P., Richter, L.J., Stan, G., Steffens, K., Zangmeister, R., Schreifels, J.A., Rao, M.V., 2012. Appl. Surf. Sci. 258, 6056–6063. https://doi.org/10.1016/j.apsusc.2012.02.137.
Xie, Q., Chen, Y., Li, X., Yin, Z., Wang, L., Geng, Y., Hong, X., 2017. Appl. Opt. 56, 1550. https://doi.org/10.1364/ao.56.001550.
Zainuddin, N.A.M., Ariannejad, M.M., Arasu, P.T., Harun, S.W., Zakaria, R., 2019. Results Phys. 13, 102255. https://doi.org/10.1016/j.rinp.2019.102255.
Zhao, Y., Lei, M., Liu, S., Zhao, Q., 2018. Sens. Actuators B Chem. 261, 226–232. https://doi.org/10.1016/j.snb.2018.01.120.